Matching and Relative Orientation of Spherical Panorama Images

Pin-Yun Chen[1] Tsung-Che Haung[2] and Yi-Hsing Tseng[3]
[1]National Cheng Kung University, No.1, Daxue Rd., East Dist., Tainan City 701, Taiwan (R.O.C.),
Email: pinyunchen@gmail.com
[2] National Cheng Kung University, No.1, Daxue Rd., East Dist., Tainan City 701, Taiwan (R.O.C.),
Email: qaz30162@gmail.com
[2] National Cheng Kung University, No.1, Daxue Rd., East Dist., Tainan City 701, Taiwan (R.O.C.),
Email: tseng@mail.ncku.edu.tw

KEY WORDS: Image Matching, Spherical Panorama Images, Essential Matrix, RANSAC

ABSTRACT: People are paying more attention to the use of Spherical Panorama Images (SPIs) for many applications. In order to apply SPIs in photogrammetric application such as land mapping or navigation like frame images do, conjugate points matching and the relative relationship between SPIs are important issues. Through observing the moving pattern of conjugate points, the relative positions and orientation between camera stations may be solved. In this study, images captured by Ladybug 5 system were used for experiment, image features were extracted and matched by Speed-Up Robust Features (SURF) algorithm (Bay, 2008), and the concept of Random Sample Consensus (RANSAC) was applied to improve the accuracy of conjugate points matching. Although RANSAC general model is not well enough to detect the features on SPIs, we proposed a method using the Essential Matrix model to improve this deficiency. Once the conjugate points are found, the relationship between image stations can be explained by Essential matrix, the rotation and translation parts can be extracted up to scale. Similar to that of frame camera, four possible solutions can be found, the angle between two image stations is used to judge the correct solution. The results show that the quantity and quality of corresponding pairs influence the accuracy of the relative positions and orientations between two images. Although the error matching pair can be found and removed by RANSAC, the distortion comes with projection still make trouble for SURF algorithm. A suitable way is apply image matching on the spherical space to improve the quality of corresponding pairs**.**

1. INTRODUCTION

1.1 Motivation and Objective

Spherical panoramic image (SPI) contains larger field of view than single frame image, we can use SPIs to get more image information, and reduce the computation cost. The applications such as multi-network adjustment and relative orientation calculation all need large amount of corresponding feature points between SPIs. In order to apply SPIs in photogrammetric application like frame images do, conjugate points matching and the relative relationship between SPIs are important issues.

Because of complex geometry of SPI, there is a problem to be solved, that is how to ensure the correctness of SPI matching. With the aid from epipolar geometry, lots of applications are proposed such as matching problem, pose problem and so on, it is widely used to establish the relationship between overlapping images. However, the approach is suitable for frame images but failure when applying SPIs since the special sphere geometry.

Corresponding to the two raised problems, there are two objectives in this study. The first one is aims at developing and implementing the theory of SPI matching. With the proposed method, we can increase the efficiency and reliability of matching result. The second one focuses on developing an algorithm to apply epipolar geometry for calculating the position and orientation of the SPIs.

1.2 Reference to Related Work

Using classical matching method for panoramic images is very challenging, they cannot provide satisfactory results in many cases, and a matching strategy using affine scale invariant features (ASIFT) was proposed to increase the feature points between overlapping omnidirectional images (Carufel, 2011).

Essential matrix plays an important role for the orientation computation in computer vision field. The minimal case solution of the essential matrix involves five 2D to 2D feature correspondences using the epipolar constraint. A simple and straightforward solution for $n \geq 8$ noncoplanar points is eight-point algorithm (Longuet-Higgins, 1981).

With these methodologies, we can compute the essential matrix and do more application (Stewenius, 2006). The relative relation between two images can be extracted from the Essential matrix. Both rotation and translation form essential matrix has two different solutions, so there are four different solutions. By triangulation of a single point, the correct pair can be identified. The four solutions are illustrated in figure 1, where it is shown that a reconstructed point will be in front of both cameras in one of these four solutions only (Hartley, 2000).

2. SPHERICAL PANORAMIC IMAGES

2.1 SPI Geometry

Usually, an SPI is generated by combining a sequence of images captured with a single camera or the images captured with a multi-camera sensor. The geometry of an SPI can be described in Fig. 2.1, where R_SPI denotes the spherical radius of an SPI, ρ denotes the zenith angle from the z-axis and α denotes the horizontal angle from the x-axis. Eq. (2.1) formulates the coordinates of an image point defined in the image frame (I-Frame).

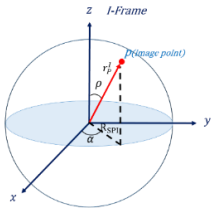

Figure 2. 1 The SPI spherical coordinate system.

$$r_P^I = \begin{bmatrix} x_p^I \\ y_p^I \\ z_p^I \end{bmatrix} = \begin{bmatrix} R_{SPI} \sin\rho \cos\alpha \\ R_{SPI} \sin\rho \sin\alpha \\ R_{SPI} \cos\rho \end{bmatrix} \quad (2.1)$$

Suppose there is an ideal SPI, the geometric relationship of an image point and the corresponding object point can be described as an image ray. When the image ray is defined in I-Frame and the corresponding object point is defined in object frame, O-Frame, the geometric relationship between the image ray and object point can be described in Fig. 2.2. It means the vector of an object point P is the combination of the vector of SPI center and the image ray. This relationship can be written as Eq. (2.2).

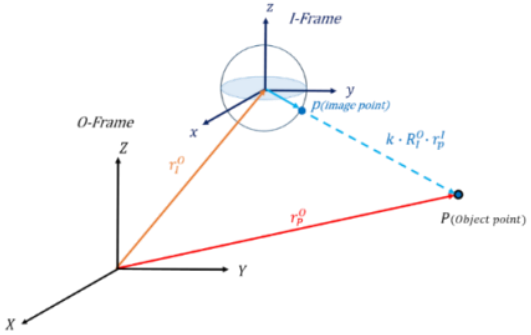

Figure 2. 2 The concept of exterior orientation of an SPI.

$$r_P^O = r_I^O + \mathrm{k} \cdot R_I^O \cdot r_P^I \quad (2.2)$$

3. IMAGE MATCHING

3.1 Speed-Up Robust Features (SURF) Algorithm

SURF is a scale-invariant and rotation invariant image matching algorithm. Bay et al. (2008) utilize Hessian matrix to detect the feature points at different scales, and utilizes the Haar wavelet responses (Lienhart et al., 2002) in x and y direction to calculate the orientation of feature points. The parameters in the algorithm can be changed in order to adapt to different cases. For example, Figure 3.1 shows the matching results with filter number 6.

3.2 Error Matching Detection and Elimination

RANSAC is an iterative method to estimate parameters of a mathematical model from a set of observed data which may contain outliers. The input of the algorithm is the matching result of SURF algorithm in this study. RANSAC achieves its goal by repeating the procedure shown in Fig 3.2. The procedure in the first dot rectangle repeat in a fixed number of times, each time produces a model. Only one model is accepted since the perfect fit with the definition expressed in Eq. (3.1) which is a matrix constraint (Stewenius et al., 2006) often used for essential matrix determination. The mathematical model plays a significant role in RANSAC algorithm. It is the criterion to distinguish between inliers and outliers from the data. The relationship between two frame images can be described by affine transformation. With this transformation relationship, the conjugate points can be filtered. This can be achieved by transforming the coordinates of one image to another as described in Eq. (3.2).

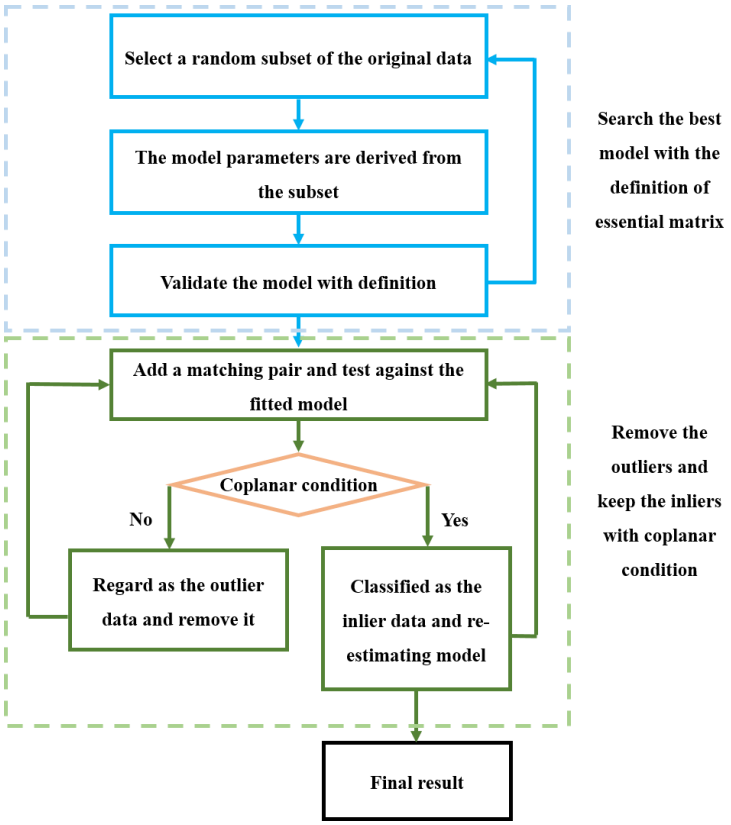

Figure 3. 1 The flow chart of RANSAC for elimination.

The geometric relationship of SPI is different with frame images. Because of the complicated geometry, affine model cannot be used for eliminating error matching. A reasonable way is finding a suitable transformation model. In this study, essential matrix is applied to be the transformation model. With the definition of essential matrix, we can ensure whether the matching pairs are correct or not, which means if the matching pair is correct, it will satisfy the coplanar condition. The transformation model is shown as Eq. (3.3).

4. RELATIVE ORIENTATION OF AN SPI PAIR

4.1 Relative Orientation

Similar to a stereo pair of frame images, the relative orientation between a pair of overlapping SPIs can be formulated and estimated with conjugate points. Relative orientation defines the position and attitude of one image with respect to the other overlapping image (Ressl, 2000). Assume there are two SPIs, the relative orientation parameters can be written as Eq. (4.1) and Eq. (4.2).

$$r^{O}_{I1\to I2} = r^{O}_{I2} - r^{O}_{I1} \tag{4.1}$$

$$R^{I1}_{I2} = R^{I1}_{O} R^{O}_{I2} \tag{4.2}$$

Both translation and rotation include three parameters, so there are totally six elements of relative orientation. However, since the uncertainty of a scale factor, the base vector between two SPIs cannot be determined and the independent parameter is only five. It means that give different scale factors, different translation parameters will be obtained. This will cause the solution infinite if there is no scale factor to be the constraint condition.

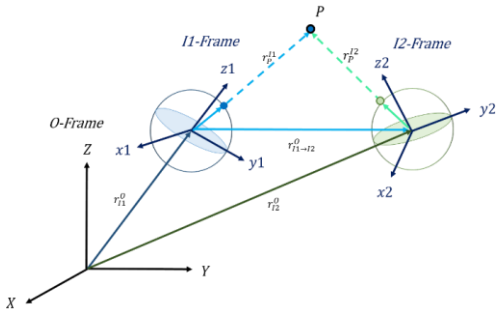

Figure 4.1 Concept of relative orientation.

4.2 Estimation of Relative Orientation

The relative orientation between two overlapped SPIs may be retrieved from the essential matrix, and scale factor can be computed by the ray intersection method with more SPIs which the E.O parameters are known. To extract the relative orientation parameters, we assume the first camera is at the origin and does not contain rotation, which means I1-Frame equals to O-Frame. The epipolar condition can be depicted in Fig 4.2, in which the volume of the parallelepiped is the scalar triple product of the three vectors, namely the image rays of two conjugate points and the base vector, is zero. The concept of coplanar condition is explained in Eq. (4.3). Essential matrix describes the relative orientation between two images (Scaramuzza, 2012). We can rewrite Eq. (4.3) into Eq. (4.4) using skew-symmetric matrix. Essential matrix is expressed as Eq. (4.5).

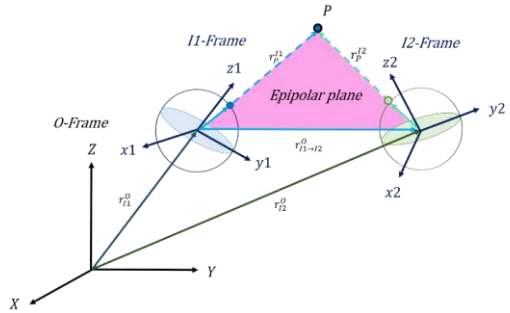

Figure 4.2 Concept of coplanar condition of SPIs.

$$(R_{I1}^{O} r_P^{I1})^T \cdot [r_{I1 \to I2}^{O} \times R_{I2}^{O} r_P^{I2}] = 0 \tag{4.3}$$

$$(r_P^{I1})^T R_O^{I1} \cdot T \cdot R_{I2}^{O} r_P^{I2} = 0 \tag{4.4}$$

where,

$T = \begin{bmatrix} 0 & -\Delta Z & \Delta Y \\ \Delta Z & 0 & -\Delta X \\ -\Delta Y & \Delta X & 0 \end{bmatrix}$: the skew-symmetry matrix of the base vector.

$$E = R_O^{I1} \cdot T \cdot R_{I2}^{O} = \begin{bmatrix} e_{11} & e_{12} & e_{13} \\ e_{21} & e_{22} & e_{23} \\ e_{31} & e_{32} & e_{33} \end{bmatrix}$$

The essential matrix can be estimated with matching image features using epipolar constraints described as Eq. (4.4). The minimal case solution involves five 2D to 2D correspondences (Nister, 2004). A simple and straightforward solution is the Longuet-Higgins' eight-point algorithm (Longuet- Hinggins, 1981) which is summarized as Eq. (4.5).

$$\begin{bmatrix} \vdots \\ x_i^{I1}x_i^{I2} \; x_i^{I1}y_i^{I2} \; x_i^{I1}z_i^{I2} \; y_i^{I1}x_i^{I2} \; y_i^{I1}y_i^{I2} \; y_i^{I1}z_i^{I2} \; x_i^{I1}z_i^{I2} \; y_i^{I1}z_i^{I2} \; z_i^{I1}z_i^{I2} \\ \vdots \\ x_n^{I1}x_n^{I2} \; x_n^{I1}y_n^{I2} \; x_n^{I1}z_n^{I2} \; y_n^{I1}x_n^{I2} \; y_n^{I1}y_n^{I2} \; y_n^{I1}z_n^{I2} \; x_n^{I1}z_n^{I2} \; y_n^{I1}z_n^{I2} \; z_n^{I1}z_n^{I2} \end{bmatrix}_{i=1\sim n} \begin{bmatrix} e_{11} \\ e_{12} \\ e_{13} \\ e_{21} \\ e_{22} \\ e_{23} \\ e_{31} \\ e_{32} \\ e_{33} \end{bmatrix} = 0 \tag{4.5}$$

Stacking the constraints from more than eight points gives the linear equation system $AE = 0$. By solving the system, the parameters of E can be computed. A valid essential matrix after SVD is $= U_E D_E V_E^T$, and has $diag(D) = \{d, d, 0\}$, which means that the first and second singular values are equal and the third one is zero. To get a valid essential matrix fulfills the constraint, the solution needs to be projected onto the space. The projected essential matrix is $\bar{E} = Udiag\{1, 1, 0\}V^T$.

However, the situation become different in SPI case. The approach for frame image is not suitable for SPI since there is no definition of front side and back side for an SPI. In this study, we proposed a novel method to deal with SPI ambiguity. Similar to the frame camera, there are four possible solutions after extracting the rotation and translation from essential matrix. The rotation and translation ambiguity for SPI is illustrated in Fig 4.3.

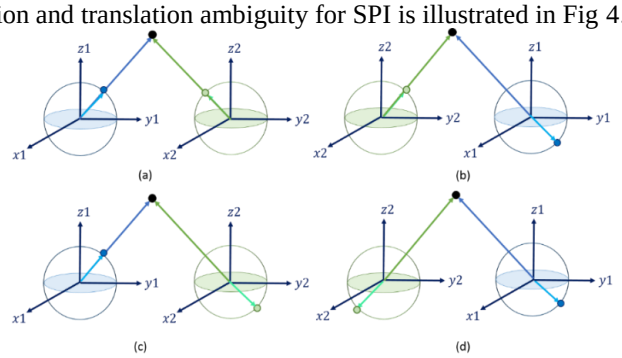

Figure 4.1 Intersection ambiguity of SPI.

Figure 4.4 shows r_P^I can be transformed into O-Frame by using rotation matrix R_I^O. Vector $r_{I\to P}^O$ also can be computed since we know the position of SPI centre and the point. If both rotation and translation of second camera are correct, the angle between $(R_I^O \cdot r_P^I)$ and $r_{I\to P}^O$ will be close to zero rather than close to 180 ˚ . We can use this check angle to solve the ambiguity of intersection. The only one correct solution is the one has the both check angles of the two SPIs to be small. The check angle of each SPI can be computed by using inner product computation.

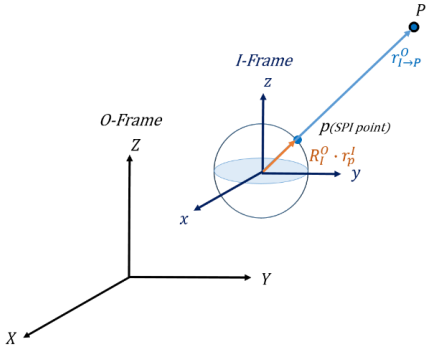

Figure 4.2 The check angle relationship for the ambiguity problem.

5. EXPERIMENT RESULT AND ANALYSIS

5.1 Essential Model Test

An experiment was conducted to compare affine and essential models for the cases of translate, rotate and tilt of the station. Each case involves several SPIs. Five images (A1~A5) were tested in the translation test; four images (B1~B4) were tested in the rotation test; and three images (C1~C3) were tested in the tilt test. Table 5.1 ~ 5.3 show the result with respect to the three test cases.

Figure 5. 1 Matching result of movement test.

(a) Affine Model (b) Essential Model

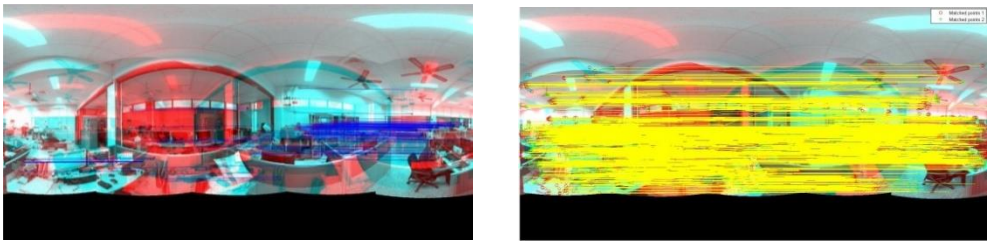

Figure 5. 2 Matching result of self-rotation test.
(a) Affine Model (b) Essential Model

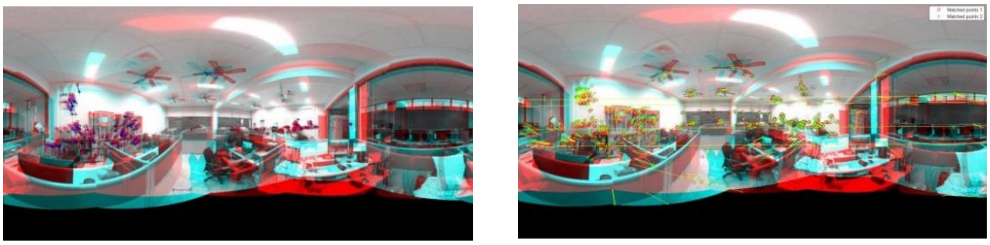

Figure 5. 3 Matching result of tilt test.
(a) Affine Model (b) Essential Model

Table 5.1 shows the numbers of points in translation test. The number of candidate points for each image pair are all more than 400. The percentages of remaining numbers of point with RANSAC affine model are about 30%. When the essential model is applied, the percentages can be increased up to about 75%.

Table 5錯誤! 所指定的樣式的文字不存在文件中。.1 Comparison of affine and essential model in movement test.

	A1A2	A2A3	A3A4	A4A5
Number of candidate matches	404	413	466	500
Number of remaining matches after RANSAC with affine model	130 (28%)	128 (31%)	139 (30%)	190 (38%)
Number of remaining matches after RANSAC with essential model	360 (77%)	335 (81%)	330 (71%)	410 (82%)

Table 5.2 shows the numbers of points in the rotation test. The numbers of candidate points for each image pair are all more than 1800. The percentages of remaining numbers of point with RANSAC affine model are about 40%, the percentages can be increased up to about 95 % using essential model.

Table 5.2 Comparison of affine and essential model in self-rotation test.

	B1B2	B2B3	B3B4	B4B1
Number of candidate matches	1888	1836	1891	1870
Number of remaining matches after RANSAC with affine model	680 (36%)	624 (34%)	794 (42%)	766 (41%)
Number of remaining matches after RANSAC with essential model	1831 (97%)	1762 (96%)	1834 (97%)	1776 (95%)

Table 5.3 shows the numbers of points in the tilt test. The numbers of candidate points for each image pair are all more than 700. The percentages of remaining numbers of point after RANSAC process with affine model are about 30%. When the essential model is applied, the percentages can be increased up to about 90%.

Table 5.3 Comparison of affine and essential model in tilt test.

	C1C2	C2C3	C1C3
Number of candidate matches	1119	1384	760
Number of remaining matches after RANSAC with affine model	358 (32%)	525 (38%)	212 (28%)
Number of remaining matches after RANSAC with essential model	1040 (93%)	1301 (94%)	554 (73%)

Although the essential model performs much better than affine model in RASNAC algorithm for SPI cases, there are still very few matched points distributed in the top and bottom area due to the serious image distortion. Even if SURF can detect the feature points in these areas, feature descriptions of these corresponding points will differ from each other, and will be removed in SURF matching. To solve the problem, it is necessary to cope with the image distortion generated by projection.

5.2 Relative Orientation Calculation Test

The indoor environment of Dept. of Geomatics contains two floors and stairs, 18 control points are measured by total station for calculating E.O. parameters of SPIs, and there are seven check points used to validate the result. Fifteen SPIs were captured using Ladybug 5 system. Fig. 5.4 shows the distribution of control points, check points and image stations. Image matching was performed to find corresponding points between two overlapped SPIs. Figure 5.5 shows the example of matching results of two SPIs, the red point means the matching feature point.

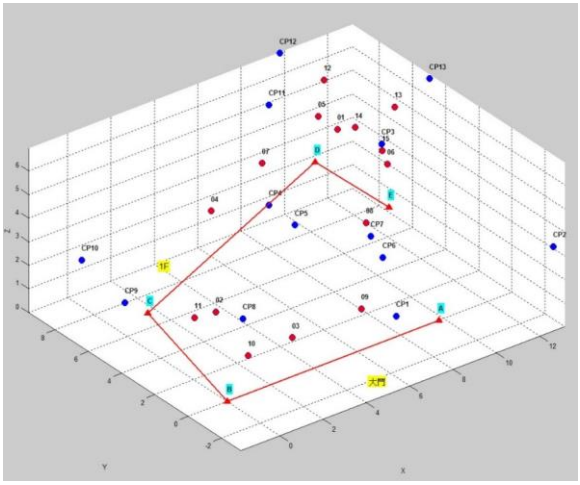

Figure 5. 4 Distribution of control points.

Figure 5. 5 SPI No. 1 match with SPI No. 14 (192 matching points)
(a) SPI No. 1 (b) SPI No. 14

Five query SPIs were chosen for testing, relative orientation parameters were computed to determine the POPs of SPIs using other ten control SPIs. Two test cases were done in this study. In test case I, manual measurements of corresponding points were applied to ensure the quality of matching pairs; the test case II is the overall test with the use of automatic measurements of corresponding points determined by SURF and RANSAC algorithm. Table 5.4 shows the difference compared to the results, also the mean errors and RMSEs.

Table 5.4 Coordinate errors and mean errors and RMSEs of case I.

	Case I			Case II		
SPI	△X(m)	△Y(m)	△Z(m)	△X(m)	△Y(m)	△Z(m)
1	-0.002	0.027	-0.004	0.011	-0.005	-0.016
2	-0.007	0.001	0.002	0.448	-0.315	0.464
3	0.045	0.007	0.014	0.216	-0.030	0.050
4	0.302	0.052	0.126	-3.654	4.090	-0.097
5	0.040	0.038	0.002	0.138	-0.276	0.060
Mean Error	0.076	0.025	0.028	0.203	-0.157	0.140
RMSE	±0.137	±0.031	±0.057	±0.258	±0.201	±0.235

The case I results show errors less than a few cm except SPI No. 4. This reveals the importance of the quality of corresponding points. The coordinate errors of SPI No. 4 are larger than the other four SPIs, especially the X coordinate. For mean error and RMSE in Case II, SPI No. 4 is not taken into account. Comparing the results of test case II with case I, coordinate error increase obviously. The much larger errors resulted from improper matching pairs of corresponding points generated from the automatic matching process. Except SPI No. 4, coordinate errors of all other SPIs are still under 1 meter.

The test of SPI No. 4 is the worst case in both Case I and Case II. In test case II, the coordinate errors even reach to four meters. By checking the distribution of control SPIs shown in Fig 5.6, SPI No. 4 locates at the stairs and there are few control SPIs around it. Table 5 shows the numbers of corresponding points between each query SPI and the top three control SPIs in the test case II. Much fewer conjugate points were found for query SPI No. 4. This reveals that the number of corresponding points also affects the positioning result. Moreover, the distribution of matched points in query SPI No. 4 is mainly on the X direction, which may cause the situation of unbalanced geometry. Based on the observations, both the quantity and the distribution of corresponding points are important factors for computation.

Table 5.5 Numbers of corresponding points between overlapped SPIs.

	Matched SPI and number of corresponding points					
SPI No. 1	SPI No. 14	297	SPI No. 5	175	SPI No. 15	91
SPI No. 2	SPI No. 11	154	SPI No. 4	33	SPI No. 9	32
SPI No. 3	SPI No. 10	149	SPI No. 9	72	SPI No. 2	46
SPI No. 4	SPI No. 1	28	SPI No. 7	22	SPI No. 10	20
SPI No. 5	SPI No. 1	191	SPI No. 14	79	SPI No. 15	60

Table 5.5 give the results of the relative rotation matrix of SPI No. 3, and the validation data are also given. By checking the results of test case I with the validation data, the calculated rotation matrix is an acceptable. For example, comparing the result of case I and case II in Table 5.6~5.8, the respective elements of computed rotation matrix are similar to those validation data, which means the result of SPI No. 3 can be considered as reasonable orientation.

Table 5.6 relative rotation matrix and rotation angles of SPI No. 3.

True value			
Rotation angle	**ω**(˚)	**φ**(˚)	**κ**(˚)
	2.09	5.34	2.05
Relative rotation matrix	0.9999500	0.0092206	-0.0024579
	-0.0092417	0.9999200	-0.0087257
	0.0023773	0.0087480	0.9999600

Table 5.7 relative rotation matrix and rotation angles of SPI No. 3.

Case I			
Rotation angle (with SPI No.10)	**ω**(˚)	**φ**(˚)	**κ**(˚)
	0.14	4.92	-8.24
Relative rotation matrix (with SPI No.10)	0.9914800	-0.1476800	-0.0888930
	0.1435900	0.9978000	0.0275950
	0.0856700	-0.0024022	0.9932500
Rotation angle (with SPI No.9)	**ω**(˚)	**φ**(˚)	**κ**(˚)
	-0.29	5.29	-7.13
Relative rotation matrix (with SPI No.9)	0.9938100	-0.1292400	-0.0944780
	0.1243800	1.0024000	0.0208890
	0.0921150	0.0050840	0.9910100

Table 5.8 relative rotation matrix and rotation angles of SPI No. 3.

Case II			
Rotation angle (with SPI No.10)	**ω**(˚)	**φ**(˚)	**κ**(˚)
	-0.13	2.18	-2.40
Relative rotation matrix (with SPI No.10)	1.0017000	-0.0416810	-0.0376630
	0.0419840	0.9999100	-0.0067668

	0.0381130	0.0022535	1.0018000
Rotation angle (with SPI No.9)	**ω**(˚)	**φ**(˚)	**κ**(˚)
	-0.95	6.10	-4.54
Relative rotation matrix (with SPI No.9)	1.0011000	-0.0829180	-0.1079900
	0.0795190	1.0013000	0.0072074
	0.1062900	0.0165310	0.9995200

6. CONCLUSION

In this study, we combined the SURF and RANSAC algorithm for searching the overlapped SPIs and measuring the corresponding image features automatically. Essential matrix which based on coplanar condition is applied in RANSAC algorithm to cope with the SPI matching process. With essential matrix model, the efficiency and reliability of matching results are more robust. Once the matching is done, the position and orientation parameters (POPs) between two overlapped SPIs can be computed with essential matrix again. A novel solution of the intersection ambiguity of SPI while calculating the relative orientation is also proposed and get a good result.

Two test cases including manual and automatic measurements of corresponding points are compared. For positioning result, using manual measurement can provide the coordinates error less than a few centimeters. About coordinate error is about twenty centimeters while using the automatic measurements. It reveals the incorrect matching pair is the main reason causing the poor position result. It means that the computation of position relies very much on the data quality of corresponding points. According to the results, fewer conjugate points will lead to an unreasonable position of unknown SPI. It means that the numbers of corresponding points also affect the positioning result.

For orientation computation, we may get reasonable results, but it may result in unreasonable numbers sometimes. The experimental results do not show a reliable and stable solution for relative rotation. At the present stage, we still cannot give a clear conclusion about why the results are unstable. What we can confirm so far is that the measurement errors of corresponding points will affect the orientation results based on the test of simulated data.

7. REFERENCE

Bay, H., T. Tuytelaars, and L. Van Gool (2008). SURF: Speeded Up Robust Features, Computer Vision and Image Understanding, 110(3), pp. 346-359.

De Carufel, J. and R. Laganiere (2011). Matching Cylindrical Panorama Sequences using Planar Reprojections, IEEE International Conference on Computer Vision Workshops, pp. 320-327.

Fischler, M.A. and R.C. Bolles (1981). Random Sample Consensus: A Paradigm for Model Fitting with Applications to Image Analysis and Automated Cartofraphy. Comm. Of the ACM, Vol. 24, pp. 381-395.

Hayet, J.B., F. Lerasle and M. Devy (2007). A visual landmark framework for mobile robot navigation. Image and Vision Computing 25, pp.1341-1351.

Hartley, R. and A. Zisserman (2004). Multiple View Geometry in Computer Vision, Cambridge Univ., pp.257-260.
Horn, B.K.P. (1990). Recovering baseline and orientation from essential matrix. MIT AI Memo.

Jyoti Joglekar and Shirish S. Gedam (2012). Area Based Image Matching Methods – A Survey. International Journal of Emerging Technology and Advanced Engineering, V ol. 2 Issue 1, pp.130-136.

Lienhart, R. and J. Maydt (2002). An Extended Set of Haar-like Features for Rapid Object Detection. IEEE ICIP, Vol. 1, pp.900-903.

Lee, Y., S. Lee, D. Kim and J.K. Oh (2013). Improved Industrial Part Pose Determination Based on 3D Closed-Loop Boundaries. IEEE International Symposium on Robotics (ISR), pp.1-3.

Longuet-Higgins, H.C. (1981). A Computer Algorithm for Reconstructing a Scene from Two Projections. Nature, 293(10), pp.133-135.

Lin, K.Y. (2014). Bundle Adjustment of Multi-station Spherical Panorama Images with GPS Positioning, Department

of Geomatics, National Cheng Kung University.

Nguyen, V.V, J.G Kim and J.W Lee (2011). Panoramic Image-Based Navigation for Smart-Phone in Indoor Environment. Springer-Verlag, Berlin Heidelberg, pp.370-376.

Nister, D. (2004). An Efficient Solution to the Five-Point Relative Pose Problem. IEEE Transaction on Pattern Analysis and Machine Intelligence, 26(6):758-759.

Ressl, C. (2000). An Introduction to the Relative Orientation Using the Trifocal Tensor. International Archives of Photogrammetry and Remote Sensing, Vol. XXXIII, Part B3:769-776.

Stewenius, H., C. Engels, D. Nister (2006). Recent Developments on Direct Relative Orientation. ISPRS Journal of Photogrammetry and Remote Sensing, 60(4), pp. 284-294.

Scaramuzza, D. and F. Fraundorfer. (2012). Visual Odometry: Part I - The First 30 Years and Fundamentals. IEEE Robotics and Automation Magazine, 18(4), pp.85-87.

Se, S., D.Lowe and J, Little (2002). Global Localization using Distintive Visual Features. IEEE/RSJ International Conference on Intelligent Robots and Systems, pp.226-231.

Wahbeh W., C. Nardinocchi (2015). Toward the Interactive 3D Modelling Applied to Ponte Rotto in Rome. Nexus Network Journal (2015), 17:55-71.

Zhang, Chi J. Xu, N. Xi, Y.Y Jia and W.X. Li (2012). Development of an Omni-direction 3D Camera for Robot Navigation. IEEE/ASME International Conference on Advance Intelligent Mechartronics, pp.262-267